Evaluation of Equivalent Spring Stiffness for Use in a Pseudo-Rigid-Body Model of Large-Deflection Compliant Mechanisms

L. L. Howell
Assistant Professor.
Mechanical Engineering Department,
Brigham Young University,
Provo, UT 84602-4138

A. Midha
Professor.
School of Mechanical Engineering,
Purdue University,
West Lafayette, IN 47907-1288

T. W. Norton
Eastman Chemical Company,
Kingsport, TN 37662

Compliant mechanisms gain some or all of their mobility from the flexibility of their members rather than from rigid-body joints only. More efficient and usable analysis and design techniques are needed before the advantages of compliant mechanisms can be fully utilized. In an earlier work, a pseudo-rigid-body model concept, corresponding to an end-loaded geometrically nonlinear, large-deflection beam, was developed to help fulfill this need. In this paper, the pseudo-rigid-body equivalent spring stiffness is investigated and new modeling equations are proposed. The result is a simplified method of modeling the force/deflection relationships of large-deflection members in compliant mechanisms. The resulting models are valuable in the visualization of the motion of large-deflection systems, as well as the quick and efficient evaluation and optimization of compliant mechanism designs.

Introduction

Compliant or flexible-link mechanisms gain some or all of their motion from the relative flexibility of their members rather than from rigid-body joints only. Compliant mechanisms have many potential advantages (Sevak and McLarnan, 1974; Salamon, 1989), e.g. reduction of the number of individual parts required, reduced weight, wear, backlash, noise, need for lubrication, and manufacturing and assembly cost and time. These advantages are seldom exploited, however, because of the complicated analysis involved in their design. The effect of energy storage in the flexible members on one hand, and nonlinearities introduced due to large elastic and rigid-body displacements of the mechanism members on the other, are major sources of these difficulties. Simple examples of compliant mechanisms are shown in Fig. 1. If not for the motion permitted by compliance in these mechanisms, each would be a structure with no mobility whatsoever.

There are several methods available that take into account the nonlinearities introduced by large deflections. A classical method, which yields a closed-form solution, involves the solution of a second-order, nonlinear differential equation using elliptic integrals (e.g., Bisshopp and Drucker, 1945; Frisch-Fay, 1962). The advantage of this solution technique is that it provides closed-form solutions. The disadvantage is that the derivations are cumbersome and solutions exist for only relatively simple geometries and loadings. Numerical methods, such as the finite element method, are capable of solving much more general problems (e.g., Yang, 1973; Bathe and Bolourch, 1979; Her, 1986). These methods are particularly useful when an initial design has been chosen, and geometry and loads are available as input to the algorithms. There is a need, however, for efficient methods which would help in arriving at these initial designs. One method is to develop an equivalent, pseudo-rigid-body model for a compliant mechanism, and use this model and knowledge of rigid-body kinematics to design the mechanism to fulfill given design requirements (Salamon, 1989). Burns (1964) and Burns and Crossley (1968) used such a method to approximate the kinematics of flexible-link mechanisms by assuming that large-deflection members transverse a path with a radius of 5/6 the member length. A pseudo-rigid-body mechanism may also model flexible members as discrete springs attached to rigid links. Howell and Midha (1994a) used such a technique to analyze compliant mechanisms with small-length flexural pivots. Since the flexural pivots considered are small in length compared to the more rigid sections, the mechanism members are essentially modeled as rigid with joints at the center of the flexural pivots. This method is not valid when the length of the flexural pivots is not small compared to the rigid sections. Therefore, a need exists for the development of a general method for synthesis of compliant mechanisms.

In an earlier paper, Howell and Midha (1995) developed a pseudo-rigid-body model for an initially straight, inextensible cantilever beam with constant cross section and linear material properties. In this work, the equivalent pseudo-rigid-body spring stiffness is studied and an alternative modeling method is presented and illustrated. The resulting model is useful in design, where many design trials are often analyzed to obtain an acceptable or optimal design. It is also useful in visualizing and predicting the behavior of large-deflection members.

Parametric Approximations

The concept of a pseudo-rigid-body model of a flexible member was presented in a recent paper (Howell and Midha, 1995), and has been shown to be a valuable tool in the analysis and design of compliant mechanisms. Figure 2 shows a single cantilevered, flexible member, Fig. 2(a) and its pseudo-rigid-body counterpart, Fig. 2(b). The model consists of two rigid links, connected by a "characteristic pivot" to represent the motion, and a nonlinear spring to model the beam stiffness or resistance to the applied force. This model predicts the deflection path of the beam end for a given end load, to within 0.5 percent of the closed-form elliptic integral solution for quite large deflections.

The method used to obtain an appropriate pseudo-rigid-body model for a given end load (Howell and Midha, 1995) begins

Contributed by the Mechanisms Committee for publication in the JOURNAL OF MECHANICAL DESIGN. Manuscript received Feb. 1994; revised Aug. 1995. Associate Technical Editor: G. R. Pennock.

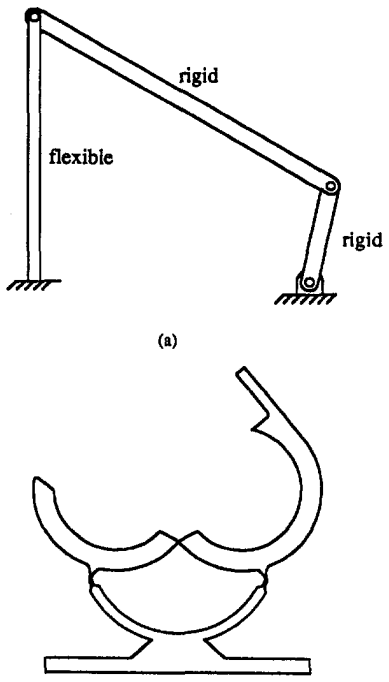

Fig. 1 Examples of compliant mechanisms

by finding the optimal location of the characteristic pivot, Fig. 2(*b*). A one-dimensional optimization routine is used to find the pivot location for which the resulting model will approximate the closed-form elliptic integral solution (deflection path) the farthest without exceeding a predetermined maximum error. The location of the pivot is expressed in terms of the "characteristic radius factor," γ, which represents the fraction of the beam length at which the pivot is located. Once γ is determined, the deflection path may be parameterized in terms of Θ, the "pseudo-rigid-body angle." Expressing the horizontal coordinate of the beam end as a, and the vertical coordinate as b, the parameterized deflection equations may be expressed as

$$\frac{a}{l} = 1 - \gamma(1 - \cos\Theta) \tag{1}$$

$$\frac{b}{l} = \gamma \sin\Theta \tag{2}$$

Considering combined end forces only, γ may be determined from the following equations (Howell and Midha, 1995):

$$\gamma = 0.841655 - 0.0067807n + 0.000438004n^2; \quad 0.5 < n < 10.0 \tag{3}$$

$$\gamma = 0.852144 - 0.0182867n; \quad -1.8316 < n < 0.5 \tag{4}$$

$$\gamma = 0.912364 + 0.0145928n; \quad -5.0 < n < -1.8316 \tag{5}$$

where n is the ratio of the horizontal force to the vertical force component, i.e., n = (horizontal force)/(vertical force), and $n > 0$ represents a horizontal force that initially causes compression. A simple rule-of-thumb for γ for use in rough calculations is $\gamma = 0.85$.

The true beam end angular deflection, θ_0, may be expressed in terms of Θ by means of a simple linear curve fit as

$$\theta_0 = c_\theta\Theta \tag{6}$$

The load-deflection relationships have also been expressed as curve fit equations. These may be summarized (Howell and Midha, 1995) as:

for $0.0 \le n \le 2.0$

$$\alpha^2 = 3.080761\Theta - 1.197269\Theta^2 - 1.324163\Theta n + 2.642665\Theta^3 - 0.702815\Theta^2 n + 0.560222\Theta n^2 - 1.615738\Theta^3 n + 0.447698\Theta^3 n^2; \quad r^2 = 0.99560 \tag{7}$$

for $-1.5 \le n \le 0.0$

$$\alpha^2 = 3.874848\Theta - 4.561288\Theta^2 - 1.244845\Theta n + 5.930629\Theta^3 + 12.131849\Theta^2 n - 0.251214\Theta n^2 - 15.288859\Theta^3 n + 22.432280\Theta^3 n^2; \quad r^2 = 0.99728 \tag{8}$$

where $\alpha^2 = Pl^2/EI$ and P is the component of the applied end force F in the vertical direction, and the correlation coefficient is given by r.

The limits of the above parametric equations may be expressed as

$$\theta_0 < \theta_{0\max} \approx 0.85 \tan^{-1}\frac{1}{-n}; \quad -5.0 < n < 10.0 \tag{9}$$

or (Norton, 1991)

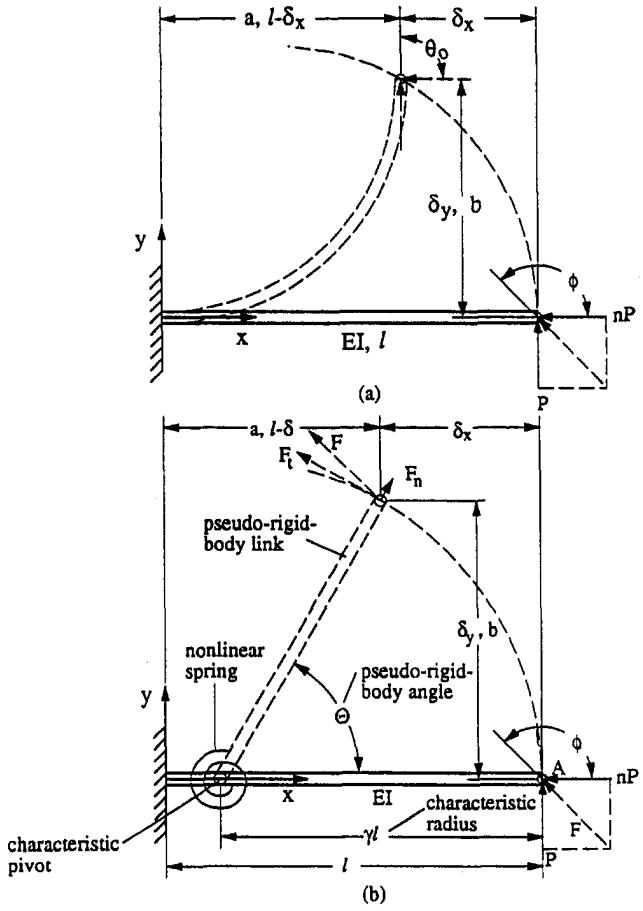

Fig. 2 (*a*) An end-force-loaded flexible cantilever segment and (*b*) its pseudo-rigid-body model

$$\Theta < \Theta_{max} \approx 0.7 \tan^{-1} \frac{1}{-n}; \quad -5.0 < n < 10.0 \quad (10)$$

Stiffness Coefficient

Further insight into the pseudo-rigid-body model and simplification may be gained by investigating the stiffness characteristics of its equivalent torsional spring (Norton, 1991). Consider the pseudo-rigid-body model of a beam shown in Fig. 2(*b*). It is reasonable to examine separately the effects of the load components F_t and F_n, tangential and normal to the path of point A, respectively. The transverse (or tangential) component of the load can be nondimensionalized as follows:

$$(\alpha^2)_t = \frac{F_t l^2}{EI} \quad (11)$$

where

$$F_t = F \sin(\phi - \Theta) \quad (12)$$

where ϕ is the angle of the applied force, as shown in Fig. 2. Figure 3 shows a plot of the nondimensionalized transverse load index, $(\alpha^2)_t$, versus the pseudo-rigid-body angle, Θ, for $n = 0$. The pseudo-rigid-body angle is calculated from

$$\Theta = \tan^{-1}\left(\frac{b}{a - l(1-\gamma)}\right) \quad (13)$$

It is interesting to note that a linear approximation of these relationships is accurate for a large range of the pseudo-rigid-body angle; the linear force-deflection relationship may be written as

$$(\alpha^2)_t = K_\Theta \Theta \quad (14)$$

where K_Θ will be referred to as the "stiffness coefficient" and can be best determined by a curve fit procedure. Therefore, the torsional spring in Fig. 2 has a constant stiffness for a given value of n. The relationship in Eq. (14) is very simple; however, it may not be accurate for the entire range of the kinematic model and the limits must be specified.

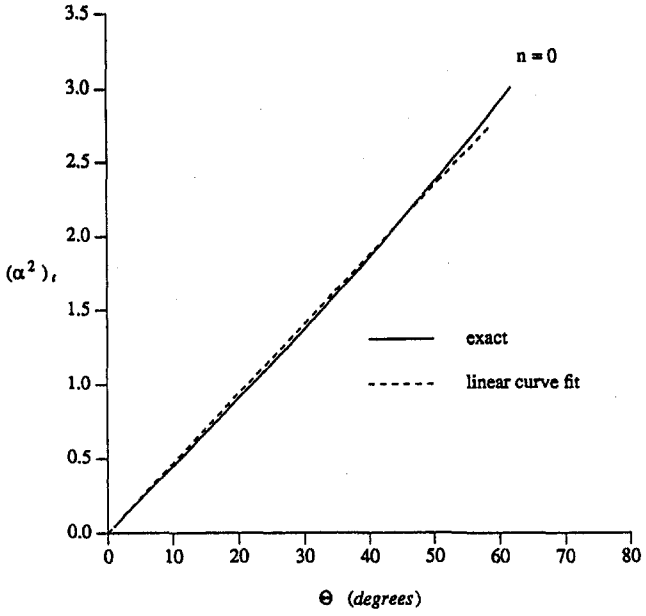

Fig. 3 Tangential force versus deflection

Table 1 Stiffness coefficients for various end loadings

n	ϕ degrees	K_Θ	r^2	Θ_{max}/ϕ	Θ_{max} degrees
-5.0	11.3	2.49874	.99978	.70	7.9
-4.5	12.5	2.54238	.99993	.70	8.8
-4.0	14.0	2.58991	.99996	.70	9.8
-3.5	15.9	2.64016	.99984	.70	11.2
-3.0	18.4	2.68893	.99949	.70	12.9
-2.5	21.8	2.74924	.99885	.70	15.3
-2.0	26.6	2.80162	.99810	.70	18.6
-1.5	33.7	2.78081	.99838	.70	23.6
-1.0	45.0	2.72816	.99891	.70	31.5
-.5	63.4	2.69320	.99893	.70	44.4
.0	90.0	2.67617	.99835	.65	58.5
.5	116.6	2.63744	.99842	.55	64.1
1.0	135.0	2.61259	.99845	.50	67.5
1.5	146.3	2.59289	.99875	.45	65.8
2.0	153.4	2.59707	.99847	.45	69.0
2.5	158.2	2.56969	.99903	.40	63.3
3.0	161.6	2.56737	.99899	.40	64.6
3.5	164.1	2.56579	.99895	.40	65.6
4.0	166.0	2.56506	.99891	.40	66.4
4.5	167.5	2.56198	.99894	.40	67.0
5.0	168.7	2.56251	.99889	.40	67.5
5.5	169.7	2.56053	.99891	.40	67.9
6.0	170.5	2.56202	.99886	.40	68.2
6.5	171.3	2.56091	.99887	.40	68.5
7.0	171.9	2.56020	.99888	.40	68.7
7.5	172.4	2.55984	.99889	.40	69.0
8.0	172.9	2.56287	.99881	.40	69.1
8.5	173.3	2.56318	.99881	.40	69.3
9.0	173.7	2.56381	.99881	.40	69.5
9.5	174.0	2.56474	.99879	.40	69.6
10.0	174.3	2.56597	.99878	.40	69.7

Values for the stiffness coefficient for several values of n are given in Table 1. These values were determined using data points at every degree of the pseudo-rigid-body angle for a given value of n. The correlation coefficient squared, r^2, is listed for each of the stiffness coefficients. The correlation coefficient can range from a value of zero, implying that there is no correlation between the curve fit and the actual relationship, to a value of one, indicating a perfect correlation. The correlation coefficient is generally assumed to be a good indicator of a curve fit if the number of data points is much greater than the order of the polynomial.

Limits for the approximation are shown (Table 1) as a ratio of the maximum pseudo-rigid-body angle, Θ_{max}, to the angle of the force, ϕ, where Θ_{max} is defined in Eq. (10). The linear approximation of Eq. (14) is not accurate for the full range of the kinematic model, as given by Eq. (10), when compressive loads ($n > 0$) are considered. However, this linearization is accurate enough over a large portion of the possible range of the pseudo-rigid-body angle, Θ.

The stiffness coefficient K_Θ is plotted as a function of n in Fig. 4. Polynomial curve fits relating the stiffness coefficient and the ratio of axial to transverse load are derived as follows:

$$K_\Theta = 3.024112 + 0.121290n + 0.003169n^2; \quad -5 < n \leq -2.5 \quad (15)$$

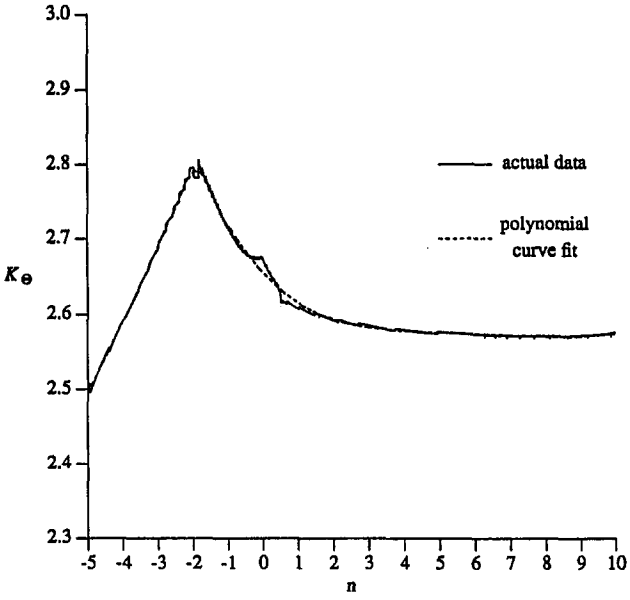

Fig. 4 Stiffness coefficient versus n

$$K_\Theta = 1.967647 - 2.616021n - 3.738166n^2 - 2.649437n^3 - 0.891906n^4 - 0.113063n^5; \quad -2.5 < n \leq -1 \quad (16)$$

$$K_\Theta = 2.654855 - 0.509896 \times 10^{-1}n + 0.126749 \times 10^{-1}n^2 - 0.142039 \times 10^{-2}n^3 - 0.584525 \times 10^{-4}n^4; \quad -1 < n \leq 10 \quad (17)$$

The correlation coefficients squared squared, r^2, for the above equations are 0.99939, 0.97786, and 0.99341, respectively. The curve fit relations given in Eqs. (15) to (17) are shown in Fig. 4.

The results in Table 1 reveal that the value of K_Θ varies by only 0.3 between its lowest and highest values for the range of loading shown. Because of this, an approximation of a constant K_Θ may be made for use in rough calculations. This may be done by calculating the average K_Θ as

$$K_{\Theta_{ave}} = \frac{\int_{n_1}^{n_2} K_\Theta dn}{\int_{n_1}^{n_2} dn} \quad (18)$$

For the load angle range $11.3° < \phi < 174.3°$, or $-5.0 < n < 10.0$, K_Θ is approximated using Eqs. (15) to (18), resulting in $K_{\Theta_{ave}} = 2.61$. Considering loads only in the most common range of $45° < \phi < 135°$, or $-0.5 < n < 1.0$, results in $K_{\Theta_{ave}} = 2.65$.

Example

Consider the compliant mechanism shown in Fig. 5(*a*). This one link mechanism is comprised of a simple fixed-pinned flexible segment, a simple fixed-fixed segment of the type described in Howell et al., 1994, a rigid segment, and ground (see Midha et al., 1994, for nomenclature). The flexible segments are made of spring steel with a modulus of elasticity, E, of 207×10^9 Pa, have a length, l, of 20 cm, a width, w, of 2.05 cm and a thickness, t, of 0.03 cm. The rigid segment also has a length, l_r, of 20 cm. The concepts described above are used to determine the deflection path of the rigid coupler and the horizontal force, P, required to obtain this motion.

The pseudo-rigid-body model for the mechanism is shown in Fig. 5(*b*) (Howell et al., 1994). The system is such that, for each segment, the changing reaction forces due to ground and the coupler yield a different value of n at each mechanism position. This variation of n through the motion causes changes in the location of the characteristic pivot and the stiffness coefficient. These changes may be accounted for in one of two ways. The simplest method is to use the averages of the characteristic radius factor, γ, and the stiffness coefficient, K_Θ, as constant values. Since the values of γ and K_Θ experience relatively small variations, their values are taken as $\gamma = 0.85$, and $K_\Theta = 2.61$. The value of the stiffness coefficient for the simple fixed-fixed segment is $2K_\Theta$, as described in Howell et al. (1994). This method is used in the example at hand to illustrate the accuracy and usefulness of even this simplified model.

The second, more accurate method requires updating the changing values of γ and K_Θ at every increment of motion using Eqs. (3) to (5), and (15) to (17). The changing values for γ results in varying link lengths in the pseudo-rigid-body model and the kinematic equations for a general four-bar linkage are required.

Assuming a constant value for γ results in a pseudo-rigid-body model that is a parallelogram mechanism, i.e., the rigid coupler remains horizontal. The displacement and required force are calculated by imposing an initial displacement on a link, calculating the resulting mechanism motion, and determining the reaction forces. The values of n for each segment are then updated and the mechanism is incremented to the next displacement.

The force-deflection relationship for the mechanism may be determined in one of several ways. It is possible to make a free

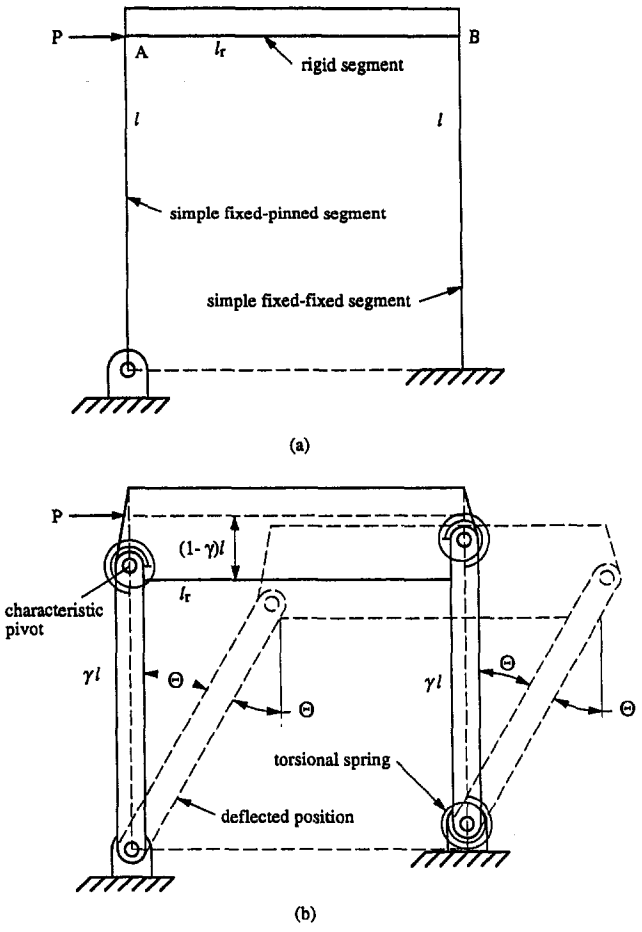

Fig. 5 (*a*) An example compliant mechanism and (*b*) its pseudo-rigid-body model

body diagram of each link of the pseudo-rigid-body model and solve for the unknown forces. An alternative method is the use of the principle of virtual work. In this method only the forces that do work are considered in the analysis. Howell and Midha (1994b) used this method to derive equations for a general pseudo-rigid-body four-bar mechanism. Using these equations, the force-deflection relationship is expressed as:

$$P = \frac{5K_\Theta EI\,\Theta}{l^2 \cos\Theta} \tag{19}$$

The path of the rigid segment in Fig. 5(*a*) is determined by Eqs. (1) and (2) and is shown plotted in Fig. 6. The results are compared to those obtained by a commercial finite element code (ANSYS) capable of large-deflection analysis. Twenty beam elements were used to model each flexural segment. The required horizontal force, P, versus horizontal deflection, Δ_x, is shown plotted in Fig. 7. These results are also compared to those obtained from the finite element solution. The results compare favorably, even for deflections out of the range recommended for K_Θ in Table 1.

The simplified model of a parallel motion mechanism and using constant values of γ and K_Θ resulted in a close approximation to the much more involved finite element solution. The accuracy of the approximation could be improved even further by allowing the values of γ and K_Θ to change throughout the mechanism motion, combined with the kinematic equations of a four-bar mechanism with arbitrary link lengths. These simplified models prove useful in visualizing the motion of large-deflection systems and predicting their behavior. They are also valuable in the initial design phase, allowing many different designs to be investigated and optimized quickly and efficiently.

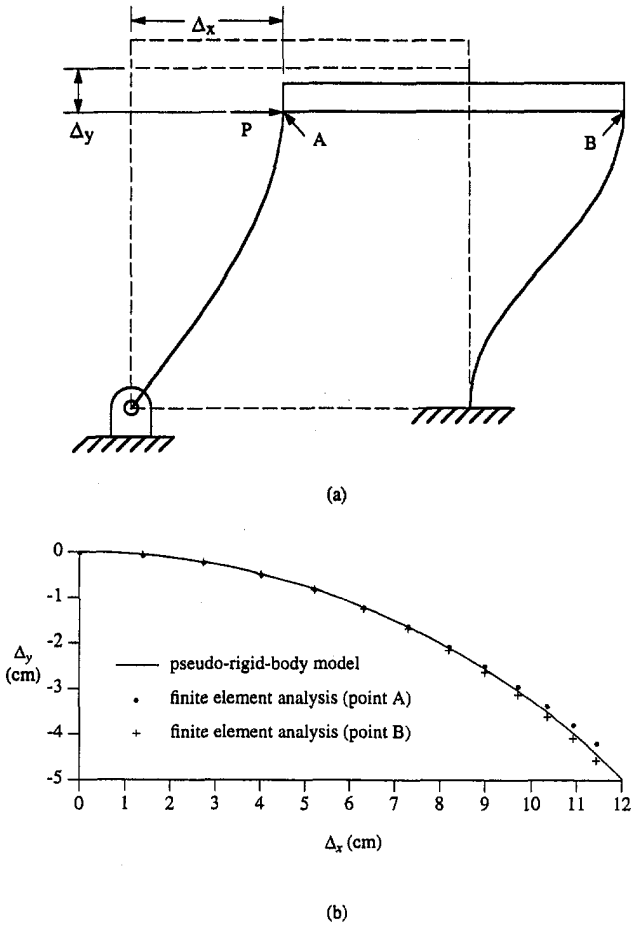

Fig. 6 (*a*) The displaced compliant parallel motion mechanism, and (*b*) the deflection path of the rigid-body segment

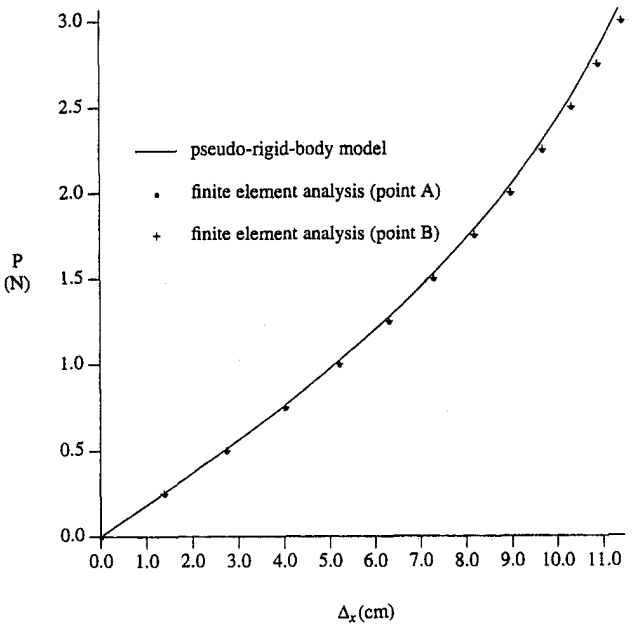

Fig. 7 Load versus deflection plot of compliant parallel motion mechanisms

Conclusion

The geometric nonlinearities involved in compliant mechanism analysis complicate the design of such mechanisms. Before the advantages of compliant mechanisms are fully utilized, more usable and reliable analysis techniques must be made available. With this goal in mind, the pseudo-rigid-body model has been developed to simplify the analysis of compliant mechanisms. The pseudo-rigid-body model is facilitated by modeling flexible members as rigid links joined at a characteristic pivot to adjoining links, and then using a standard rigid-body kinematic analysis method to analyze the compliant mechanism. This paper extends an earlier work, wherein a pseudo-rigid-body model is developed for an initially straight, end-force loaded cantilever member, to now include simplified approximations for the force-deflection characteristics by means of the stiffness coefficient. An example mechanism was also analyzed to illustrate the application of the concepts introduced herein to compliant mechanism analysis. The resulting models are useful in visualizing the motion of large-deflection members, and in the quick and efficient evaluation and optimization of compliant mechanisms.

References

Bathe, K.-J., and Bolourch, S., 1979, "Large Displacement Analysis of Three-Dimensional Beam Structures," *International Journal For Numerical Methods in Engineering*, Vol. 14, pp. 961–986.

Bisshopp, K. E., and Drucker, D. C., 1945, "Large Deflection of Cantilever Beams," *Quarterly of Applied Mathematics*, Vol. 3, No. 3, pp. 272–275.

Burns, R. H., 1964, "The Kinetostatic Synthesis of Flexible Link Mechanisms," Ph.D. Dissertation, Yale University.

Burns, R. H., and Crossley, F. R. E., 1968, "Kinetostatic Synthesis of Flexible Link Mechanisms," ASME Paper No. 68-Mech-36.

Frisch-Fay, R., 1962, *Flexible Bars*, Butterworth, Washington, D.C.

Her, I., 1986, "Methodology for Compliant Mechanism Design," Ph.D. Dissertation, Purdue University.

Howell, L. L., 1993, "A Generalized Loop-Closure Theory for the Analysis and Synthesis of Compliant Mechanisms," Ph.D. Dissertation, Purdue University.

Howell, L. L., and Midha, A., 1994a, "A Method for the Design of Compliant Mechanisms with Small-Length Flexural Pivots," ASME JOURNAL OF MECHANICAL DESIGN, Vol. 116, No. 1, pp. 280–290.

Howell, L. L., and Midha, A., 1994b, "The Development of Force-Deflection Relationships for Compliant Mechanisms," *Machine Elements and Machine Dynamics,* G. R. Pennock, ed., DE-Vol. 71, 23rd ASME Mechanisms Conference, pp. 501–508.

Howell, L. L., Midha, A., and Norton, T. W., 1994, "Evaluation of Equivalent Spring Stiffness for Use in a Pseudo-Rigid-Body Model of Large-Deflection Compliant Mechanisms," *Mechanism Synthesis and Analysis,* G. R. Pennock, ed., DE-Vol. 70, 23rd ASME Mechanisms Conference, pp. 405–412.

Howell, L. L., and Midha, A., 1995, "Parametric Deflection Approximations for End-Loaded, Large-Deflection Beams in Compliant Mechanisms," ASME JOURNAL OF MECHANICAL DESIGN, Vol. 117, No. 1, pp. 156–165.

Midha, A., Norton, T. W., and Howell, L. L., 1994, "On the Nomenclature, Classification, and Abstractions of Compliant Mechanisms," ASME JOURNAL OF MECHANICAL DESIGN, Vol. 116, No. 1, pp. 270–279.

Norton, T. W., 1991, "On the Nomenclature and Classification, and Mobility of Compliant Mechanisms," M.S. Thesis, Purdue University.

Salamon, B. A., 1989, "Mechanical Advantage Aspects in Compliant Mechanisms Design," M.S. Thesis, Purdue University.

Sevak, N. M., and McLarnan, C. W., 1974, "Optimal Synthesis of Flexible Link Mechanisms with Large Static Deflections," ASME Paper No. 74-DET-83.

Yang, T. Y., 1973, "Matrix Displacement Solution to Elastica Problems of Beams and Frames," *International Journal of Solids and Structures,* Vol. 9, No. 7, pp. 829–842.